ANALYSIS OF NEAR FIELD BROADBAND PIC ANTENNA ARRAY PROCESSOR WITH ORTHOGONAL INTERFERENCE BEAM

Md Rakibul Islam and Mark C Reed

School of Engineering and Information Technology
The University of New South Wales, Canberra, ACT 2600, Australia
Emails: M.R.Islam@unsw.edu.au and Mark.Reed@unsw.edu.au

ABSTRACT

A Postbeamformer Interference Canceler (PIC) is a beam space processor that processes the signals derived from an array of antennas by forming a signal beam and an interference beam. The paper presents a PIC processor using the orthogonal interference beam (OIB) and studies its performance by deriving the analytical results for the output signal to interference plus noise ratio (SINR) when an array is situated in the near field of broadband directional sources. A number of examples are presented to support the analytical results.

Index Terms— Smart antennas, near field PIC processor, orthogonal interference beam, broadband array processing

1. INTRODUCTION

Most of the literature assumes that the array is situated in the far field of the directional sources and thus plane wave propagation is assumed. There are circumstances where the sources are located very close to the array and the assumption of plane wave propagation results in errors. These situations arises, for example, in the application of microphone arrays to mobile telephony, video or teleconferencing in small enclosures where the source is located in the array's near field and the spherical wave propagation is applicable as discussed in [1–11] and references therein.

The majority of array literature using PIC processor deals with far field case only as discussed in [12–17]. This paper proposes a method by extending the technique of [12, 13] to study the performance of PIC processor when an array is situated in near field of broadband acoustic sources. The work [12] discusses narrowband and [13] discusses broadband with plane wavefront by considering only the directions of the sources. While the present study is related to the model of near field broadband with spherical wavefront where the directions and distances are considered in all derivations. The proposed method processes signals, after transforming the received broadband signals using DFT, at each frequency bin over the band of interest using narrowband PIC with OIB.

The contribution of this paper is to introduce a new method using OIB with projection technique for near field broadband PIC processor. It derives the analytical expression for output SINR by considering two scenarios a) direction of arrival (DOA) and b) distance discrimination. The processor does not require the steering delays as usually is the case for broadband beamforming [18]. A number of examples are presented to verify the theoretical results.

The paper is organized as follows: In the next section the near field signal model is discussed. Section 3 contains the proposed method. Derivation and analysis are provided in Section 4. Results and discussion are included in Section 5 and Section 6 concludes the paper.

2. NEAR FIELD SIGNAL MODEL

For an array of identical omnidirectional elements in the near field of M uncorrelated sources, let the origin of the coordinate system be taken as the time reference as illustrated in Fig. 1(A). Thus the time taken by a spherical wave arriving from the i^{th} source in the direction (θ_i, ϕ_i) situated at a distance r_i and measured from the ℓ^{th} element to the origin is given by

$$\tau_{i\ell}(r_i, \theta_i, \phi_i) = \frac{|\underline{d}_i - \underline{d}_\ell| - |\underline{d}_i|}{c} \tag{1}$$

with $\underline{d}_i = r_i[\hat{x} \quad \hat{y} \quad \hat{z}][\cos\theta_i \sin\phi_i, \sin\theta_i \sin\phi_i, cos\phi_i]^T$ denoting the position vector of the i^{th} source, $\underline{d}_\ell$ similarly denoting the position vector of ℓ^{th} element and c is the speed of propagation of the spherical wavefront.

In this paper, two scenarios a) DOA and b) distance discrimination are considered using a uniform linear array (ULA) geometry with element spacing d whose elements are positioned along the x-axis such that the first element is situated at the origin as shown in Fig. 1(B).

Consider an array of L isotropic elements emerged in the near field of two uncorrelated broadband acoustic sources plus uncorrelated background noise. One source is the desired signal source located at (r_S, θ_S) and the other one is an undesirable interference at (r_I, θ_I). Let the induced signals on the array elements be denoted by an L dimensional vector $\underline{x}(t)$, given by

$$\underline{x}(t) = [x_1(t), x_2(t), \ldots, x_L(t)]^T \tag{2}$$

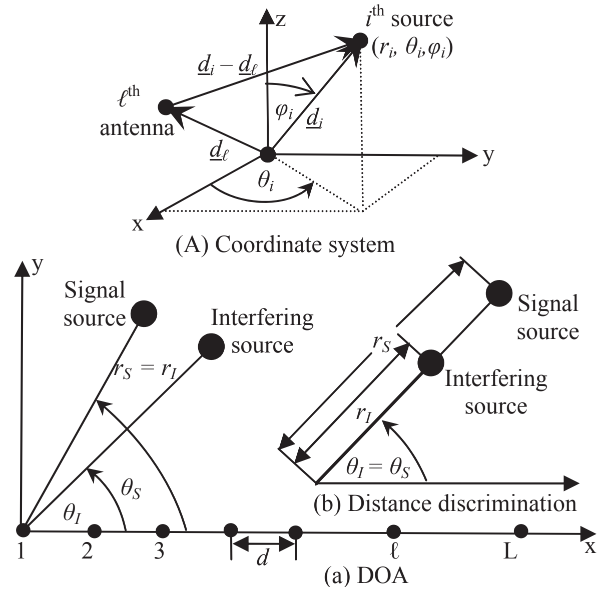

(B) ULA geometry with two scenarios (a) and (b)

Fig. 1. Near field model.

with $x_\ell(t)$ denoting the signal induced on the ℓ^{th} array element and the superscript T denotes the transpose of a vector or a matrix.

Accounting for the fact that the magnitude of a spherical wave falls off as $\frac{1}{r}$ and energy falls off as $\frac{1}{r^2}$, assuming that the ℓ^{th} element is situated at a distance of $r_{i\ell}$ from the i^{th} source, $x_\ell(t)$ is given by [3]

$$x_\ell(t) = \sum_{i=1}^{M} \frac{r_i}{r_{i\ell}} s_i(t - \tau_{i\ell}) + n_\ell(t), \tag{3}$$

where $n_\ell(t)$ denotes the random noise component on the ℓ^{th} element and $s_i(t)$ denotes the signal of the i^{th} source.

Let the induced signals be sampled at the sampling frequency f_S. Let an LN dimensional vector $\underline{X}(t)$ denote N sampled signals. It is given by

$$\underline{X}(t) = [\underline{x}^T(t), \underline{x}^T(t-T), \ldots, \underline{x}^T(t-(N-1)T)]^T \tag{4}$$

where sampling interval $T = \frac{1}{f_S}$.

Let an $LN \times LN$ dimensional matrix R denote the array correlation matrix given by

$$R = E[\underline{X}(t)\underline{X}^T(t)]. \tag{5}$$

The correlation between two signals from channel ℓ and k before m^{th} and n^{th} delay respectively, for the i^{th} source of autocorrelation $\rho_i(\tau)$, is given by [3]

$$(R_{m,n})_{\ell,k} = \frac{r_i^2}{r_{i\ell} r_{ik}} \rho_i((m-n)T + \tau_{i\ell} - \tau_{ik}), \tag{6}$$
$$\ell, k = 1, 2, \cdots, L; \quad m, n = 1, 2, \cdots, N,$$

where $r_{i\ell}$ and r_{ik} denote the distances from the i^{th} source to ℓ^{th} and k^{th} element respectively.

Let $\widetilde{R}_{nf}(k)$ denote the near field array correlation matrix at the k^{th} bin given by

$$\widetilde{R}_{nf}(k) = E[\underline{\widetilde{x}}(k)\underline{\widetilde{x}}^H(k)] \tag{7}$$

where $\underline{\tilde{x}}(k)$ denote the signals at k^{th} bin after using DFT and the superscript H denotes the Hermitian transpose of a matrix or a vector.

It can be shown that R and $\widetilde{R}_{nf}(k)$ are related by [19]

$$\widetilde{R}_{nf}(k)_{\ell i} = \underline{e}^H(k)(R_{\ell i})\underline{e}(k), \quad \ell, i = 1, ...L \tag{8}$$

where

$$\underline{e}(k) = \frac{1}{N}\left[1, \cdots, e^{-j(\frac{2\pi}{N})mk}, \cdots, e^{-j(\frac{2\pi}{N})(N-1)k}\right]^T. \tag{9}$$

3. PROPOSED METHOD

The structure of the near field PIC processor at the k^{th} frequency bin is shown in [1]. The output $q(k)$ of the near field processor in vector notation is given by

$$q(k) = \underline{V}^H(k)\underline{\widetilde{x}}(k) - w(k)\underline{U}^H(k)\underline{\widetilde{x}}(k), \tag{10}$$

where $\underline{V}(k)$ and $\underline{U}(k)$ denote L dimensional complex weight vectors for signal and interference beams respectively.

The mean output power of the processor for a given $w(k)$ is given by

$$\begin{aligned} P(w(k)) = E[q(k)q^*(k)] &= \underline{V}^H(k)\underline{\widetilde{R}}_{nf}(k)\underline{V}(k) + w^* w \\ &\quad \underline{U}^H(k)\underline{\widetilde{R}}_{nf}(k)\underline{U}(k) - w^*\underline{V}^H(k)\underline{\widetilde{R}}_{nf}(k)\underline{U}(k) \\ &\quad - w\underline{U}^H(k)\underline{\widetilde{R}}_{nf}(k)\underline{V}(k). \end{aligned} \tag{11}$$

The optimal weight which minimizes $P(\underline{w}(k))$ is given by

$$\hat{w}(k) = \frac{\partial P(\underline{w}(k))}{\partial w(k)} = 0 \tag{12}$$

which along with (11) implies that

$$\hat{w}(k) = \frac{\underline{V}(k)\widetilde{R}_{nf}(k)\underline{U}(k)}{\underline{U}^H(k)\widetilde{R}_{nf}(k)\underline{U}(k)}. \tag{13}$$

In this paper the signal beam weight $\underline{V}(k)$ is formed as

$$\underline{V}(k) = \underline{S}_0(k)/L \tag{14}$$

with $\underline{S}_0(k)$ denoting the near field steering vector associated with the desired signal position at k^{th} frequency bin given by

$$(\underline{S}_0(k))_\ell = \frac{r_s}{r_{\ell s}} e^{j2\pi(k/N)f_S(\tau_{\ell s} - \tau_s)} \tag{15}$$

where $r_{\ell s}$ and r_s respectively denote the distances from the desired signal position to the ℓ^{th} element and reference point, $\tau_{\ell s}$ and τ_s denote the propagation delays from the desired position to the ℓ^{th} element and reference point respectively.

The interference beam weights of the near field processor are selected as [12]

$$\underline{U}(k) = P(k)\underline{S}_I(k) \tag{16}$$

where $P(k)$ is a projection matrix given by

$$P(k) = I - \underline{S}_0(k)\underline{S}_0^H(k)/L \tag{17}$$

with I denoting an identity matrix and $\underline{S}_I(k)$ denoting the steering vector associated with the near field undesired interference position at k^{th} frequency bin.

4. DERIVATION OF ANALYSIS

In this section analytical expressions for the mean output signal power, interference power and the noise power at various frequency bins for near field processor are derived to study their behavior and to show how these quantities vary as a function of relative positions of two broadband acoustic sources, their power and background noise level.

In [12, 13] the PIC processor for far field model is analyzed where only the direction of the sources is considered. We significantly modify this to take into account for the near field system model, in all the derivations we consider the directions and distances. The mean output signal power $P_S(k)$, interference power $P_I(k)$ and noise power $P_n(k)$ for near field processor are derived as

$$P_S(k) = p_S(k),\ P_I(k) = \frac{p_I(k)[1-\xi(k)]}{[1+\gamma(k)(Lp_I/\sigma_n^2(k))]^2} \tag{18}$$

$$P_n(k) = \frac{\sigma_n^2(k)}{L}\left[1 + \frac{(1-\xi(k))\gamma(k)}{(\gamma(k)+(\sigma_n^2(k)/Lp_I))^2}\right] \tag{19}$$

with $p_S(k)$, $p_I(k)$ and $\sigma_n^2(k)$ denoting the input power spectral densities of signal, interference and background noise at the k^{th} bin respectively,

$$\xi(k) = 1 - \underline{S}_0^H(k)\underline{S}_I(k)\underline{S}_I^H(k)\underline{S}_0(k)/L^2 \tag{20}$$

and

$$\gamma(k) = \frac{\underline{U}^H(k)\underline{S}_I(k)\underline{S}_I^H(k)\underline{U}(k)}{L\underline{U}^H(k)\underline{U}(k)}. \tag{21}$$

Let $\Omega(k)$ denote the output SINR of the near field processor at the k^{th} bin. When the interference beam is formed by (16), it can easily be shown that $\gamma(k) = \xi(k)$ and it follows from (18) and (19) that

$$\Omega(k) = \frac{P_S(k)}{P_I(k)+P_n(k)} = \frac{Lp_S(k)}{\sigma_n^2(k)}\left[\frac{\xi(k)+\frac{\sigma_n^2(k)}{Lp_I(k)}}{1+\frac{\sigma_n^2(k)}{Lp_I(k)}}\right]. \tag{22}$$

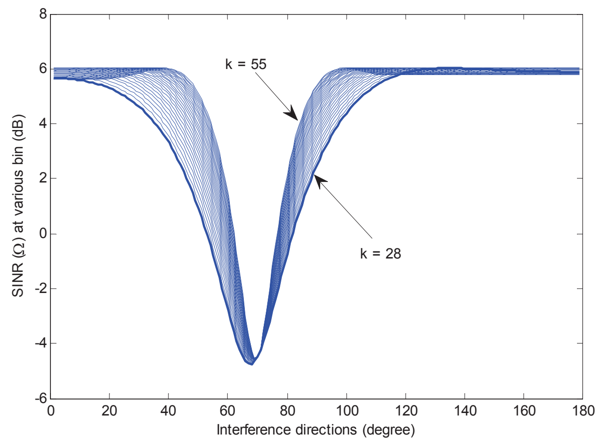

Fig. 2. SINR $\Omega(k)$ versus interference directions with $L = 4$, $N = 125$, $r_S = r_I = 5\lambda_H$, $\theta_S = 70^0$, $\theta_I = [0 - 180^0]$, $p_S(k) = p_I(k) = \sigma_n^2(k) = 1$ and bandwidth=[0.22 - 0.44].

From (22) it can be seen that the results of the processor not only depend on spectral densities of noise, interference and signal, $\Omega(k)$ also depends upon $\xi(k)$ which in turn depends upon array geometry and positions of two sources. Plots of $\Omega(k)$ for various interference directions and distances are shown in Figs. 2 and 3 respectively for an equispaced array of 4 elements with half wavelength (λ_H) spacing at highest frequency using $N = 125$ and signal bandwidth from bin 28 to 55 corresponding to normalized frequency [0.22 - 0.44].

Fig. 2 shows $\Omega(k)$ as a function of interference DOAs when signal source makes an angle of 70^0 with the line of the array and coming from the same distance as that of the interference of $5\lambda_H$. One observes from the figure that when θ_S is close to θ_I, $\Omega(k)$ is very small. As θ_S moves away from θ_I, $\Omega(k)$ varies monotonically with k whereas when θ_S is far away from θ_I, $\Omega(k)$ attains the highest value and the variation with k is not monotonical.

Fig. 3 shows $\Omega(k)$ as a function of interference distances when signal source is assumed to be situated at a distance of $5\lambda_H$ away from the reference point and coming from the same direction as that of the interference. One observes from this figure that it agrees with the results of Fig. 2, $\Omega(k)$ depends upon the distance of the interference. For example when r_I is at about $6\lambda_H$, $\Omega(k)$ increases monotonically between about 0.4 to 5.2 dB whereas when r_I is at about $2\lambda_H$ the variation with k is not monotonical.

5. RESULTS AND DISCUSSION

The analytical derivation for the output SINR $\Omega(k)$ assumes that the sources are sinusoidal at the k^{th} bin. This implies an assumption of infinite samples for broadband sources whereas when N is finite the SINR at the k^{th} frequency bin is given

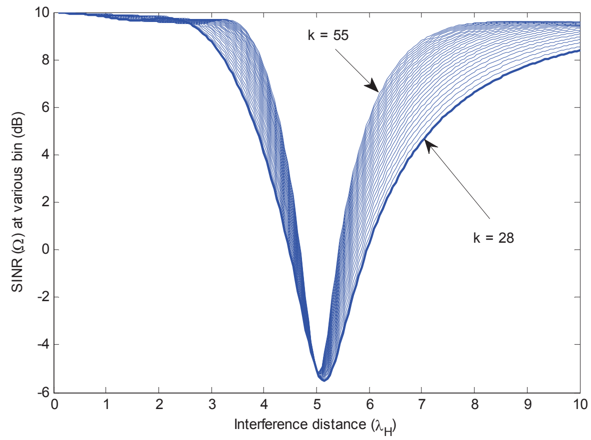

Fig. 3. SINR $\Omega(k)$ versus interference distances with $L = 4$, $N = 125$, $r_S = 5\lambda_H$, $r_I = [0 - 10]\lambda_H$, $\theta_S = \theta_I = 70^0$, $p_S(k) = p_I(k) = \sigma_n^2(k) = 1$ and bandwidth=[0.22 - 0.44].

by

$$\text{SINR}(k) = \frac{P_S(\hat{w}(k))}{P_I(\hat{w}(k)) + P_n(\hat{w}(k))} \tag{23}$$

with $P_S(\hat{w}(k))$, $P_I(\hat{w}(k))$ and $P_n(\hat{w}(k))$ denoting the mean output signal, interference and background noise power given by (11) for given $\hat{w}(k)$. It should be noted that in the limit as $N \to \infty$, $\Delta f = \frac{1}{N} \to 0$, i.e. each bin becomes a sinusoid and thus SINR(k)$\to \Omega(k)$.

In this section a number of examples are presented to show the effect of various parameters on the results. The results are obtained by computer simulation for the configurations used in the previous section.

Fig. 4 shows SINR(k) and $\Omega(k)$ as a function of bin numbers for different interference DOAs for the same configuration of Fig. 2.

One observes from Fig. 4 that the analytically derived value of the SINR at the kth bin is higher than the actual value for the finite bandwidth scenario and almost the same when $\theta_I = 60^0$. The SINR increases with k for interference DOAs of 60^0 and 85^0 whereas for 140^0 the SINR is almost constant with k. The processor has also less SINR when the interference is closer to the signal source. These are expected from the variation in $\Omega(k)$ shown in Fig. 2 and from inspection of (22). This confirms the analytical study in the previous section that the output SINR varies with k and the variation depends upon the relative DOAs of two sources.

It is also observed that an increase in number of samples makes the simulation results closer to the analytical ones as expected and the figure is not shown here.

Fig. 5 shows SINR(k) and $\Omega(k)$ for different interference locations for the scenario of Fig. 3. One observes from this figure that it agrees with the results of Fig. 4 and confirms the theoretical results that the output SINR varies with k and the variation depends upon the distances of the two sources.

It is also observed that for small σ_n^2, $\Omega(k) \propto \xi(k)$ and the SINR is very small for large σ_n^2. These are expected from studying (22).

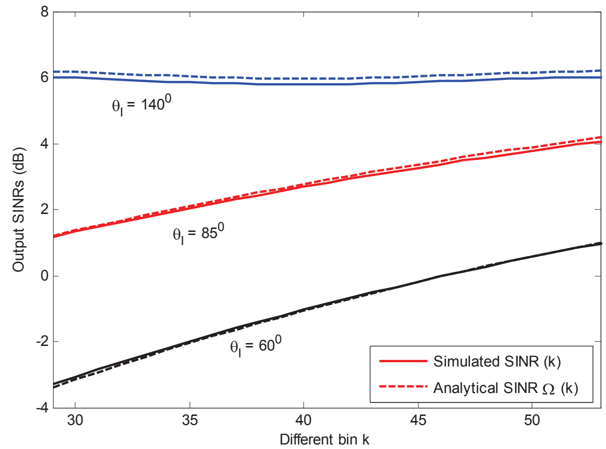

Fig. 4. Output SINRs versus bin numbers for different interference directions for the same configuration of Fig. 2.

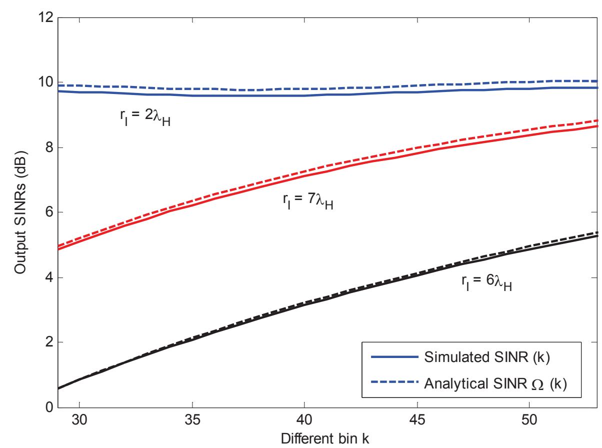

Fig. 5. Output SINRs versus bin numbers for different interference distances for the scenario of Fig. 3.

6. CONCLUSION

This paper has presented for the first time a method to analyze the performance of PIC processor for near field broadband acoustic sources by deriving expressions for output SINR. It has discussed how the results are affected by various parameters especially the relative positions of two sources and has been compared to simulation results. A close match has been achieved between the two cases.

7. REFERENCES

[1] M. R. Islam, M. C. Reed, and G. N. Milford, "Near field broadband PIC processor with improved interference beam," in *Proc. 12th Int. Symp. Comms. and Information Tech. (ISCIT)*, Oct. 2012, pp. 132 –137.

[2] M.R. Islam, L.C. Godara, and M.S. Hossain, "Robust near field broadband beamforming in the presence of steering vector mismatches," in *Proc. IEEE 13th Annual Wireless and Microwave Technology Conference (WAMICON)*, April 2012, pp. 1 –6.

[3] M.R. Islam, L.C. Godara, and M.S. Hossain, "A computationally efficient near field broadband beamformer," in *Proc. IEEE Latin-American Conference on Communications (LATINCOM)*, Oct. 2011, pp. 1 –5.

[4] L.Yan-ping, J.Yan-min, and Z.Chao-zhu, "Robust near-field beamforming with worst case performance based on convex optimization," in *Proc. 5th Global Symposium on Millimeter Waves (GSMM)*, May 2012, pp. 608 –611.

[5] D. Masovic and M. Adnadevic, "Experimental verification of near-field beamforming using low-cost microphone array," in *Proc. 19th Telecommunications Forum (TELFOR)*, Nov. 2011, pp. 1044 –1047.

[6] F. Viola, M.A. Ellis, and W.F. Walker, "Time-domain optimized near-field estimator for ultrasound imaging: Initial development and results," *IEEE Trans. on Medical Imaging*, vol. 27, no. 1, pp. 99 –110, Jan. 2008.

[7] Y.R. Zheng, P. Xie, and S. Grant, "Robustness and distance discrimination of adaptive near field beamformers," in *Proc. IEEE Int. Conf. on Acoustics, Speech and Signal Proces. (ICASSP)*, May 2006, vol. 4, pp. 1041–1044.

[8] R. Tulpule, N. Karnik, B.P. Kumar, and G.R. Branner, "Experimental study of near-field beamforming in conformal k-band linear arrays," in *Proc. IEEE Int. Symp. on Antennas and Propagation Society*, June 2003, vol. 3, pp. 268 – 271.

[9] N.Yousefian, A.Akbari, and M.Rahmani, "Using power level difference for near field dual-microphone speech enhancement," *Applied Acoustics*, vol. 70, no. 1112, pp. 1412 – 1421, 2009.

[10] Y.R. Zheng, R.A. Goubran, and M. El-Tanany, "Robust near-field adaptive beamforming with distance discrimination," *IEEE Trans. on Speech and Audio Processing*, vol. 12, no. 5, pp. 478 – 488, Sep. 2004.

[11] Q. Zeng and D. O'Shaughnessy, "Optimum design of near-field sensor arrays," in *Proc. IEEE Int. Symp. on Antennas and Propagation Society*, 2002, vol. 2, pp. 140 – 143.

[12] L.C.Godara, "Postbeamformer interference canceler with improved performance," *The Journal of the Acoustical Society of America*, vol. 85, no. 1, pp. 202–213, 1989.

[13] L.C. Godara and P. Israt, "Study of broadband post-beamformer interference canceler antenna array processor using orthogonal interference beamformer," in *Proc. 17th IEEE Int. Conf. on Electronics, Circuits, and Systems (ICECS)*, Dec. 2010, pp. 794 –797.

[14] K.Yang, D.Zhang, B.Lei, and Y.Ma, "Robust linear matched field processor based on environmental perturbation in shallow water," in *Proc. IEEE Int. Symp. on Antennas and Propagation Society*, July 2006, pp. 3387 –3390.

[15] K.Yang, Y.Ma, and S.Yan, "Robust matched field noise suppression for towed line array," in *Proc. MTTS/IEEE TECHNO-OCEAN*, Nov. 2004, vol. 2, pp. 1037 – 1041.

[16] M.H. Er, "A new approach to the design of postbeamformer interference canceller," in *Proc. Engineering in the Ocean Environment (OCEANS'90)*, Sep. 1990, pp. 512 –517.

[17] A.Cantoni and L.C.Godara, "Performance of a post-beamformer interference canceller in the presence of broadband directional signals," *The Journal of the Acoustical Society of America*, vol. 76, no. 1, pp. 128–138, 1984.

[18] O.L. Frost, "An algorithm for linearly constrained adaptive array processing," *Proceedings of the IEEE*, vol. 60, no. 8, pp. 926 – 935, Aug. 1972.

[19] L.C. Godara, *Smart Antennas*, CRC Press, 2004.